16th World Conference on Earthquake, 16WCEE 2017

Santiago Chile, January 9th to 13th 2017

Paper N° 2122

Registration Code: S-U1463307372

ENERGY DISSIPATOR STEEL CUSHIONS: CLOSED FORM EQUATIONS FOR THE COMBINING ACTIONS

A. Güllü(1), E. Yüksel(2), H. F. Karadoğan(3)

(1) *PhD Candidate, İstanbul Technical University, Department of Civil Engineering, ahmetgullu@itu.edu.tr*
(2) *Assoc. Prof. Dr., İstanbul Technical University, Department of Civil Engineering, yukselerc@itu.edu.tr*
(3) *Prof.Dr. İsik University, Department of Civil Engineering, karadogan@itu.edu.tr*

Abstract

Earthquakes impart significant amount of energy into the structures. The input energy is dissipated by the plastic deformation of structural members in the conventional design practice. Nevertheless, the input energy can be dissipated by using additional damping devices and hence the damage can be transferred from the structural members to the energy dissipaters.

A novel energy dissipater device produced by bending of mild steel has been developed in Structural and Earthquake Laboratory (STEELab) of Istanbul Technical University within the framework of FP7: SAFECLADDING Project. The behaviors of cushions have been determined by uni-axial and bi-axial loading tests as well as the finite element models which were prepared in ABAQUS.

The closed form equations for the combining shear and axial force effects have been drived by using the classical flexibility method to define load carrying capacity of P_u, yield displacement of δ_y and ultimate displacement of δ_u. Accuracy of the closed form equations is evaluated not only comparing with the test results but also the numerical results obtained from the ABAQUS models for varying cushion dimensions. An acceptable correlation is obtained between the results of the closed form equations and the numerical as well as the experimental studies.

Keywords: energy dissipation, steel cushions, closed form equation

1. Introduction

Input energy imparted by the seismic actions may be dissipated through the energy dissipative devices placed in specific locations in the structural systems instead of plastic deformation of primary structural members. Moreover, displacement and acceleration demands of the structural system can be reduced by supplied additional damping which result in smaller internal forces also.

Energy dissipative devices may be classified such as metallic dampers, friction dampers, viscous dampers etc. according to their dissipation mechanism. The steel cushion is a kind of metallic damper and it mitigates the seismic energy by means of yielding and large plastic deformation capabilities of mild steel. There is considerable amount of research on different metallic dampers because of their low-cost and easy accessibility. Kelly et al. (1972) showed that U strip type steel elements might be an important energy mitigation source by the performed experiments. U strip type steel elements were placed between adjacent walls to dissipate energy in the content of Precast Seismic Structural Systems (PRESSS), [2]. Steel slit damper produced from a standard wide-flange section was tested by Chan and Albermani, [3]. It was investigated the effect of geometric parameters of the device. It reaches the yielding at small deformation amplitude, and it results in dissipating considerable amount of energy. Henry et al. (2010) proposed an energy dissipative connector to use between adjacent walls. Although connectors dissipate considerable amount of energy, out of plane deformations were observed during the tests. The performance of the pipe type dampers with and without concrete fill and dual pipe type dampers were investigated by Maleki et al. [5] and [6]. Experimental results yield that unfilled device has a better potential to dissipate energy then the concrete filled pipe damper. Furthermore, strength, stiffness and energy dissipation capacity of the dual pipe damper exceeds two individual pipe dampers. FEMs were used to investigate the size effect on pipe dampers. FEA shows energy dissipation capability of the pipe dampers related with the length and thickness of the devices. Baird et al. (2013) utilized U–shaped flexural plates (USPs) in the cladding connections. They performed tests and analytical studies to investigate the energy dissipation capacity of the suggested device. Induced earthquake energy is dissipated by the flexural yielding properties of the device. The force-displacement hysteresis derived from the component tests were compared with the analytical results to simulate the hysteretic behavior of the USP cladding connections. The study showed that USP has a high energy dissipation capability as a passive energy dissipative device. Besides, the numerical study showed that the peak stress values in the transition part of the device is in accordance with the experimental studies. Gray et al. (2014) generated yielding brace system for the concentrically braced frames. The system dissipates seismic energy by yielding of the fingers in a special casted steel connector. Geometry of the device is evaluated by using the nonlinear FEA.

In the current study, behavior of an innovative energy dissipative device namely steel cushion, which is developed within the framework of SAFECLADDING project, is investigated analytically and numerically under effect of the combined loading. Additionally, closed form formulations were derived for load carrying capacity P_u, yield displacement δ_y, and ultimate displacement δ_u by means of classical flexibility method and virtual work theorem. Analytical studies are performed by using ABAQUS v14.1, [9]. The analytical and numerical backbone curves are compared with the cyclic experimental results. Even though U-shaped dampers are existing in the literature, the suggested steel cushion has a unique geometry which provides larger capacities due to the collaboration of the sections.

Steel cushion is connected to the testing set-up by bolts. The connection may be deliberated by using diverse bolt configurations to increase its effectiveness. Shear behavior of steel cushion was presented elsewhere [10, 11, 12, 13] both experimental and analytical aspects. The axial behavior is expressed in [14] in the analytical manner. Therefore, this paper is a complementary work of the research.

2. Steel Cushion and Experimental Study

Geometry of steel cushion consists of two half circles and a straight part. Radius of the tested specimens is 50 mm and length of straight part is 150 mm. Total length and width of specimens are 250 and 100 mm, respectively. Three diverse plate thicknesses were utilized for the specimens namely 3, 5 and 8mm. Geometric properties of the 8 mm thick specimen are shown in Fig.1.

A special testing set-up is designed in STEELab for the combined actions of axial and shear forces. A vertically oriented MTS servo-hydraulic actuator forced the cushion to generate shear displacements while constant axial load was supplied by the horizontally oriented hydraulic jack, Fig. 1. The testing protocol was created in accordance with the FEMA 461.

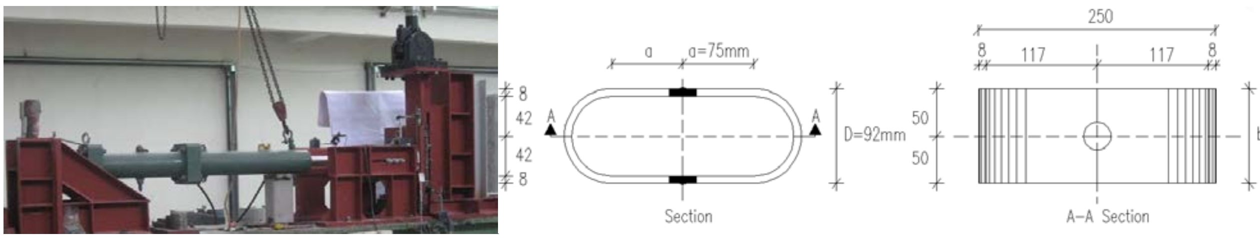

Fig. 1 – Specially designed testing set- up and typical steel cushion

Details of the experimental study can be found elsewhere, Yüksel et al. (2016), [15].

3. Finite Element Models

FEMs are generated by using ABAQUS v14.1 (ABAQUS Inc. 2014) to simulate the experiments and reproduce the experimental results analytically. Coupon tests of steel cushion were conducted to define material properties in detail. Obtained nominal stress vs. strain curves converted into true stress vs. true strain relations. *Kinematic hardening* is used to represent post-yield behavior of mild steel as it is clarified in *ABAQUS Users' Manuel*.

Simplified FEMs are generated which have 325 nodes and 260 S4R shell elements. These shell elements use *reduce integration* technique and *hourglass control* which reduce the computational costs. Additionally, S4R shell elements are able to capture local buckling. Two rigid walls at each side of steel cushion generated to represent possible boundary conditions in practice. One of the walls is completely fixed while the other one transmits the forces to steel cushion. The steel plates having 20 mm thickness created washer effects inside the cushion. *Tie contact* is used between the inner plate and inner surface of cushion and outer surfaces of cushion and free wall. *Kinematic coupling* is an efficient property of ABAQUS to reduce post-processing efforts. Fig.2 illustrates the finite element model and the deformations.

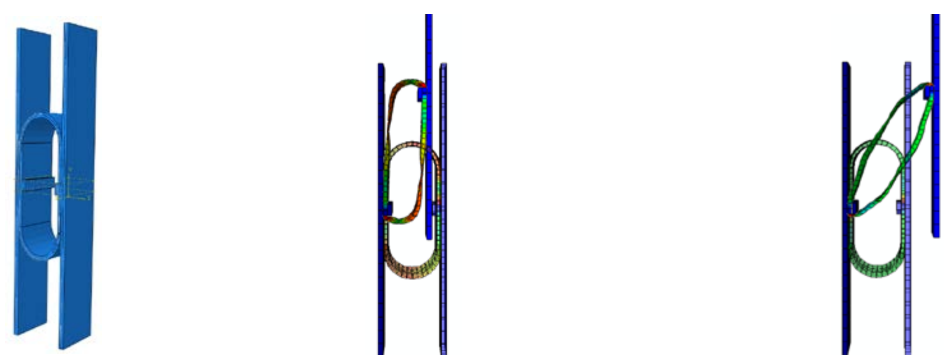

a- FEM　　b- Shear case under compression　　c- Shear case under tension

Fig. 2 – FEA of steel cushion

Numerically (FEA) obtained backbone curves are compared with the hysteresis of experiments in Fig.3.

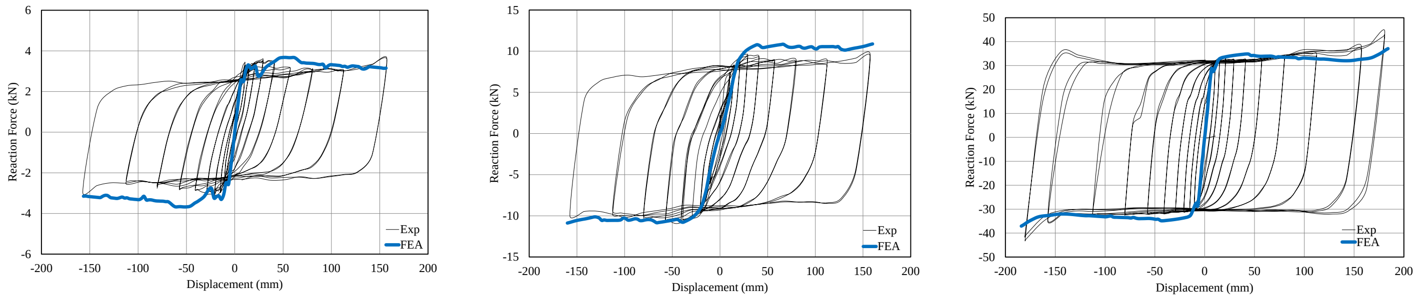

t=3mm 2.5kN tensile load   t=5mm 7.5kN tensile load   t=8mm 25kN tensile load

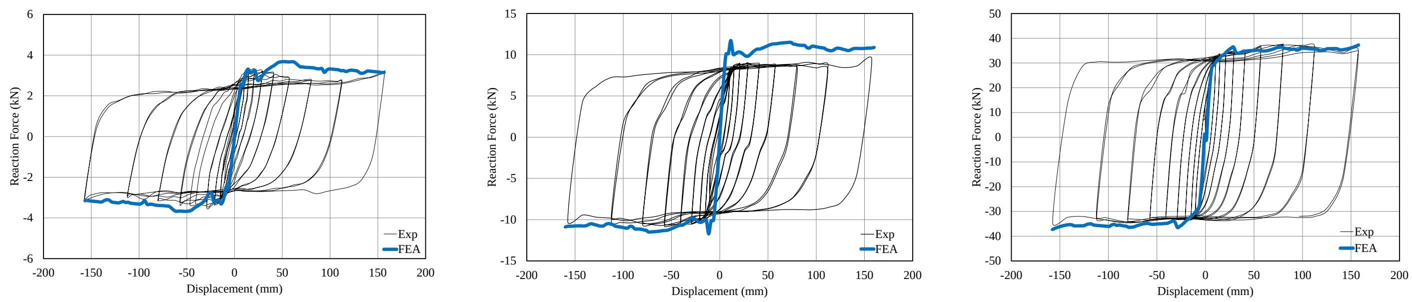

t=3mm 2.5kN compressive load   t=5mm 7.5kN compressive load   t=8mm 25kN compressive load

Fig. 3 – Comparison of experimental and numerical results for assorted thicknesses

4. Derivation of the Closed Form Solutions for Combined Loading

The equations of steel cushion for the effect of combined loading is determined through flexibility method and post-yield behavior. Essential parameters to define steel cushions are (r) radius of the half circle, (a) half length of the straight part, (t) plate thickness, (b) width of cushion, (φ) angle between the top point of half circle and any point on the circle. In addition to those parameters, ($\varphi_{\max}$) express the location of maximum moment occurred on the circular part, (D) is distance between the straight parts and ($\bar{D}$) is distance between the centers of the plasticized sections, Fig.4.

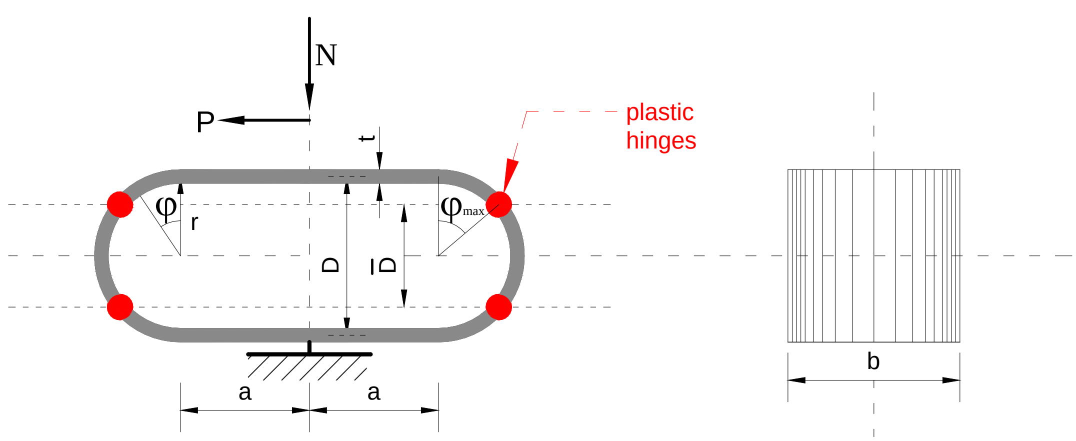

Fig. 4 – Essential parameters for steel cushion

Shear force capacity (P_u) of the steel cushion can be calculated by means of virtual work theorem, Eq. (1).

$$P_u = \frac{f_{yd} b t^2}{2r\cos\varphi_{\max}} \tag{1}$$

The steel cushion has three redundancies in flexibility method for the given support condition, see Fig. 4. Redundant forces are selected by cutting the straight part and they are nominated as X_1, X_2 and X_3, Fig. 5. Homogenous solutions for the unknown forces are obtained by considering the unit values of them.

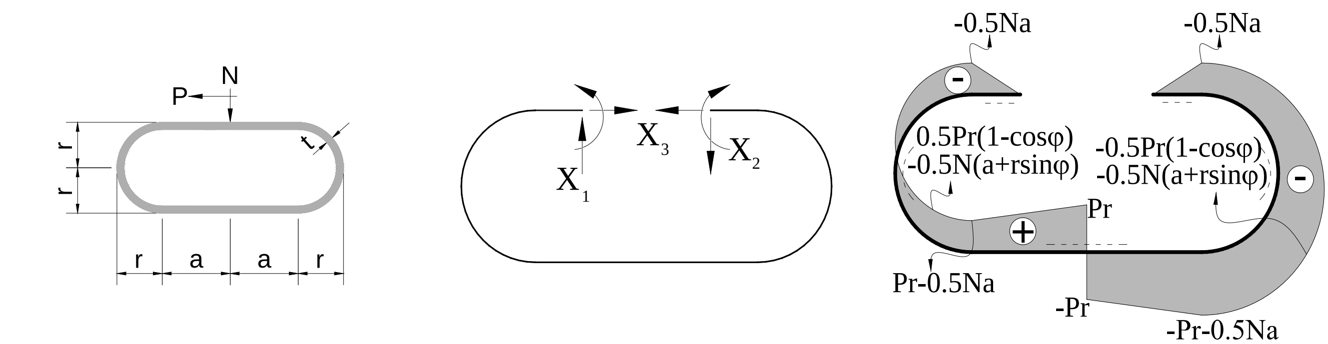

Loading | Redundant forces | Particular solution (M_0)

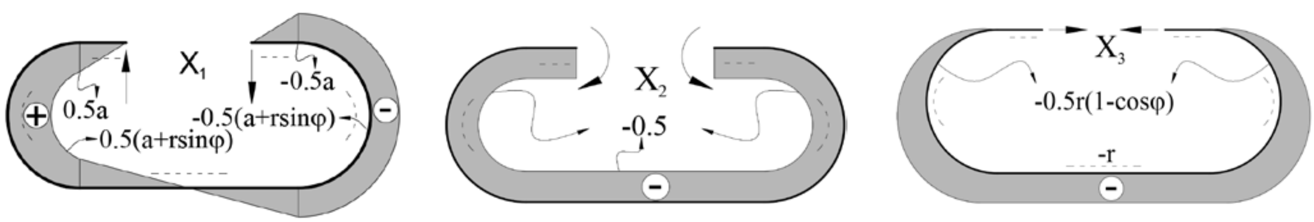

Homogeneous solution for X_1 (M_1) | Homogeneous solution for X_2 (M_2) | Homogeneous solution for X_3 (M_3)

Fig. 5 – Particular and homogeneous solutions for flexibility method

Compatibility equations are determined by means of the particular and homogenous solutions, Eqs. (2, 3).

$$\begin{aligned}\delta_{10} + \delta_{11}X_1 + \delta_{12}X_2 + \delta_{13}X_3 = 0\\ \delta_{20} + \delta_{21}X_1 + \delta_{22}X_2 + \delta_{23}X_3 = 0\\ \delta_{30} + \delta_{31}X_1 + \delta_{32}X_2 + \delta_{33}X_3 = 0\end{aligned} \tag{2}$$

$$\delta_{ii} = \int \frac{M_i M_i}{EI} ds \qquad \delta_{ij} = \int \frac{M_i M_j}{EI} ds \tag{3}$$

Redundant internal forces can be obtained from Eq. (2) as given in Eq. (4).

$$X_1 = -\frac{6\,\mathrm{Pr}\left(a^2 + \pi ar + 2r^2\right)}{4a^3 + 6\pi a^2 r + 24ar^2 + 3\pi r^3} \quad X_2 = \frac{N\left(a^2 + \pi ar + 2r^2\right)}{2a + \pi r} \quad X_3 = 0 \tag{4}$$

Bending moment diagram can be generated by using the calculated redundant forces, Eq. (5). Derivation of the moment function yields shear force distribution and location of zero shear corresponds to ultimate moments Eq. (6).

$$M(\phi)=\frac{N}{2}\left(\frac{2r^2-a^2}{2a+\pi r}-r\sin\varphi\right)-\frac{Pr}{2}\left((\cos\varphi-1)+\frac{6(a+r\sin\varphi)(a^2+\pi ar+2r^2)}{4a^3+6\pi a^2r+24ar^2+3\pi r^3}\right) \tag{5}$$

$$\varphi_{\max}\longrightarrow T(\varphi)_{\max}=\frac{dM(\varphi)}{d\varphi}=0 \tag{6}$$

The implicit equations for horizontal and vertical displacements are derived through virtual work theorem Eqs. (7, 8).

$$\delta_h=\frac{Pr^2}{EI}\left(\frac{5a^4+9\pi a^3r+(36+1.5\pi^2)a^2r^2+12\pi ar^3+(2.25\pi^2-12)r^4}{4a^3+6\pi a^2r+24ar^2+3\pi r^3}\right) \tag{7}$$

$$\delta_v=\frac{Nr}{2EI}\left(\frac{\pi a^3+8a^2r+2\pi ar^2+(\pi^2-8)r^3}{2a+\pi r}\right) \tag{8}$$

Load carrying capacity and location of maximum moment are dependent to each other, so that there is a necessity to apply an iterative process to find the solution. Initially, load carrying capacity should be calculated by Eq. (1) by considering the term of $\cos\varphi$ is equal to 0.75, then location of maximum moment and vertical displacement can be found by Eq. (6) and Eq. (8), respectively. In the subsequent steps, P_u can be calculated by using the $\varphi_{\max}$ found in the previous step and $\bar{r}=r-\delta_v/2$. This process will be continued till the results of two consecutive steps closed enough to each other. The convergence rate of the process is very high and one can reach the solution mostly in three or four steps.

Ultimate shear displacement capacity of the steel cushion is directly related with length of the straight part of steel cushion and it is defined in Eq. (9)

$$\delta_u=2a \tag{9}$$

Comparison of the experimental hysteresis with the backbone curves obtained from the closed form solutions (CFS) are presented in Fig. 6. There is an acceptable accordance between the experimental and analytical results.

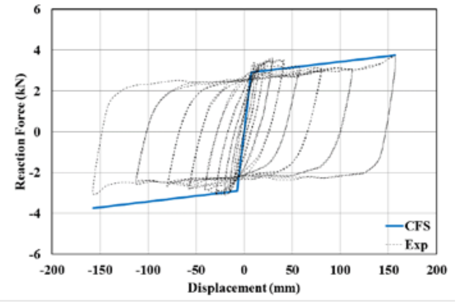

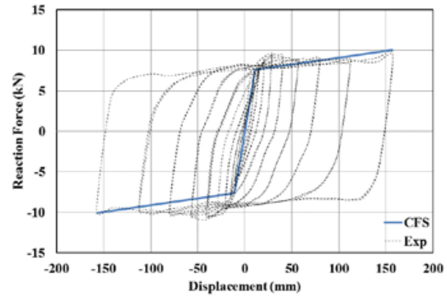

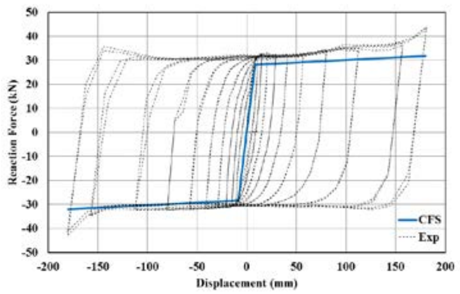

t=3mm 2.5kN tensile load | t=5mm 7.5kN tensile load | t=8mm 25kN tensile load

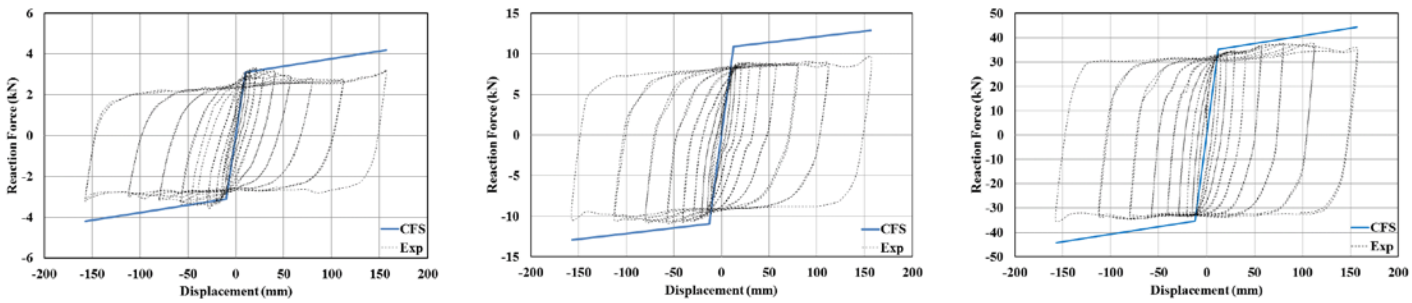

t=3mm 2.5kN compressive load | t=5mm 7.5kN compressive load | t=8mm 25kN compressive load

Fig. 6 – Experimental hysteresis vs. CFS results

5. Conclusions

The energy dissipative steel cushions which are engineered and produced in STEELab have a giant potential to mitigate large amount of input energy imparted to the structure from the seismic events either uni-axial or bi-axial loading cases. In this study, effect of the combined actions is investigated. The following results may be driven,

- The load carrying capacity of the steel cushion highly depends on the axial load direction. Compressive axial loads increase the capacity of cushion while the tensile ones decrease it.
- Finite element modeling experience gained in this study can be extended to steel cushions with dissimilar geometry. Calibration of the model with the experimental hysteresis was an essential step to resolve the converge matter.
- Numerical backbone curves practically envelope the experimental hysteresis.
- Backbone curves obtained through the closed form equations have an acceptable agreement with the experimentally obtained hysteresis.
- A design engineer can predict the load carrying capacity, yield displacement and ultimate displacement of a steel cushion by means of the derived closed form equations.

6. Acknowledgements

The research presented herein was conducted in the framework of the FP7 project "*SAFECLADDING: Improved Fastening Systems of Cladding Wall Panels of Precast Buildings in Seismic Zones*" Research for SME Associations, Grant Agreement number 314122, which was coordinated by Dr. Antonella Colombo from ASSOBETON, Italy. The financial support provided by the Commission of the European Communities through this project is greatly appreciated.

7. References

[1] Kelly JM, Skinner RI, Heine AJ (1972): Mechanisms of energy absorption in special devices for use in earthquake resistant structures. Bulletin of the New Zealand Society for Earthquake Engineering 5(3).

[2] Priestley MJN, Sritharan S, Conley JR, Pampanin S (1999): Preliminary results and conclusions from the PRESSS five-story precast concrete test-building. PCI Journal, Vol. 44(6), pp. 42-67.

[3] Chan RW, Albermani F (2008): Experimental study of steel slit damper for passive energy dissipation. Engineering Structure, 30(4), 1058-66.

[4] Henry RS, Aaleti S, ASCE S, ASCE JM (2010): Concept and finite-element modelling of new steel shear connectors for self-centering wall systems. Journal of Engineering Mechanics. doi:10.1061/_ASCE_EM.1943-7889.0000071.

[5] Maleki S, Bagheri S (2010): Pipe damper, Part I: Experimental and analytical study. Journal of Constructıon Steel Research, 66: 1088-1095.

[6] Maleki S, Mahjoubi S (2013): Dual-Pipe damper. Journal of Constructional Steel Research 2013, 85: 81–91.

[7] Baird A, Palermo A, Pampanin S (2013): Controlling seismic response using passive energy dissipating cladding connections. *New Zealand Society for Earthquake Engineering Conference,* Christchurch, New Zealand, 2013.

[8] Gray MG, Christopoulos C, Packer JA (2014): Cast steel yielding brace system for concentrically braced frames: Concept development and experimental validations. ASCE Journal of Structural Engineering, 140(4). Doi:10.1061/(ASCE)ST.1943-541X.0000910.

[9] ABAQUS (2014). ABAQUS standard manual Version 6.14, FEA: Providence, RI, USA.

[10] Smyrou E, Güllü A, Yüksel E, Özkaynak H, Karadoğan HF (2014): Modelling of an energy dissipator for precast RC cladding systems. *2nd European Conference on Earthquake Engineering and Seismology*, Istanbul, Turkey.

[11] Özkaynak H, Güllü A, Gökçe T, Khajehdehi A, Mahdavi M, Azizisales F, Bal İE., Smyrou E, Yüksel E, Karadoğan HF (2014): Energy dissipative steel cushions, *2nd European Conference on Earthquake Engineering and Seismology*, Istanbul, Turkey.

[12] Güllü A, Özkaynak H, Khajehdehi A, Gökçe T, Azizisales F, Bal İE, Smyrou E, Yüksel E, Karadoğan HF (2015): Derivation of the closed form equations for the energy dissipative steel cushions, *14th World Conference on Seismic Isolation, Energy Dissipation and Active Control of Structures*, San Diego, CA., USA.

[13] Özkaynak H, Güllü A, Khajehdehi A, Gökçe T, Azizisales F, Bal İE, Smyrou E, Yüksel E, Karadoğan HF (2015): Bi-directional loading tests of steel cushions, *14th World Conference on Seismic Isolation, Energy Dissipation and Active Control of Structures*, San Diego, CA., USA.

[14] Güllü A, Yüksel E, Khajehdehi A, Karadogan HF, Özkaynak H (2016): Experimental and analytical evaluation of the axial behavior of energy dissipative steel cushions, *New Zealand Society for Earthquake Engineering, Conference*, Christchurch, New Zealand.

[15] Yüksel E, Karadoğan HF, Özkaynak H, Khajehdehi A, Güllü A, Bal IE, Smyrou E (2016): Behavior of steel cushions subjected to the combined actions. *Under review*.